Mechanics of Advanced Composite Structures 8 (2021) 235-244

Mechanics of Advanced Composite Structures

Semnan University

journal homepage: http://MACS.journals.semnan.ac.ir

Size-dependent Vibration Analysis of Non-uniform Mass Sensor Nanobeams

M. Nazemizadeh [a]*, H. Saffari [a], A. Assadi [a], M. Taheri [b]

[a] *Faculty of Mechanics, Malek Ashtar University of Technology, Iran*
[b] *Department of Mechanical Engineering, Faculty of Engineering, Arak University, Arak, Iran*

KEYWORDS

Nanobeam
Vibration
Mass sensor
Size effects

ABSTRACT

In the present paper, the exact modeling and frequency analysis of the mass sensor nanobeam are investigated based on a higher-order elasticity theory with taking into account the longitudinal discontinuity. The energy equations of the beam are expressed considering discontinuity, and finally, the vibration equations and boundary conditions of the non-uniform nanobeam are derived using Hamilton's principle. By the implementation of an analytical solution, the number of shape functions equal to longitudinal discontinuities is assumed. Then, by expressing the compatibility and boundary conditions, the frequency equation of the discontinuous nanobeam is obtained and solved. Effects of different parameters such as sensed mass and size effects on the frequency behavior of the nanobeam are investigated at various vibrational modes. The results show that accurate modeling of discontinuous nanobeam is important. Also, Changing the position of the sensed mass to the free end of the nanotube increases the sensing feature of the beam, and the size effect reduces it. The size effect reduces the frequency and increases the amplitude of the mode shape, especially at higher vibrational modes. The results also show that the sensing feature of the mass sensor nanobeam is more prominent at higher modes of vibration, and therefore the use of mass sensor nanobeam at higher vibrational modes is recommended.

1. Introduction

Recent advances in manufacturing technologies have made it possible to develop small-scale systems at micron/submicron scales. In recent decades, nanostructure technologies have enabled the development and application of advanced micro/nanosystems, such as atomic force microscopes (AFMs), nanoactutors, nanosensors, etc. [1-3]. In fact, the nano-scale beams possess prominent features such as small dimensions, easy manufacturing, and high-frequency performance which make them the main components of nanosystems.

Furthermore, most of the nanobeams operate in vibrational or dynamic modes. Therefore, the dynamic analysis of nanobeams has attracted the attention of many researchers in the field of nanotechnology.

Taheri [4] studied sensitivity analysis of dimensional parameters on dynamic behavior of carbon nanotubes. Also, Korayem et al. [5] studied dynamic modeling of an atomic force nanomechanical beam adjacent to a surface considering tip-sample interaction forces. They introduced the critical force and time as important parameters of the performance of atomic force microscopes nanobeam and carried out the sensitivity analysis of dimensions of the nanobeam such as length, thickness, and height on its dynamic behavior. However, they modeled the system as a lumped mass, which cannot be approved as an accurate model for a continuous beam, especially in the nano-scale.

In the previous studies, the classic elasticity theory has been used to derive the dynamic equations of nanobeams, although the ability of this theory to dynamically describe the micro/nanosystems is strongly doubted through conducting experimental tests and molecular simulations [6-7]. Indeed, the mechanical properties and behavior of micro/nanobeams depend on their dimensions at small scales, which the classical theory of elasticity is unable

* Corresponding author. Tel.: +98-9127376322 ; Fax: +98-3145227136
E-mail address: nazemi@ mut-es.ac.ir

DOI: 10.22075/MACS.2021.20648.1267
Received 20-06-17; Received in revised form 21-01-20; Accepted 21-04-01

to consider. Besides, performing experimental tests at micro/nano-scales is challenging and costly. Thus, in the past few decades, size-dependent theories of elasticity have been presented for the dynamic analysis of small-scale systems and have attracted many researchers in the field of nanoscience. Jiang and Yan [8] employed the surface elasticity theory for the mechanical analysis of nanobeams, which is known as a higher-order elasticity theory. They derived the governing vibration equation of the nanobeam by employing the surface elasticity theory. Also, in [9], vibration analysis of carbon nanobeams was performed for virus detection with consideration of the surface elasticity theory. Jalali et al. [10] investigated the size-dependent vibration of a functionally graded micro-resonator based on the modified couple stress theory. They employed the Rayleigh-Ritz method to obtain the size-dependent natural frequencies of the beam for different boundary conditions. Khorshidi and Fallah [11] presented size-dependent vibration of a functionally graded nanostructure considering modified couple stress theory. Also, they [12] investigated temperature distribution and size effects on vibration behavior of such nanostructures undergoing prescribed overall motion. They developed vibration equations of the nanostructure-based on modified couple stress theory and exponential shear deformation theory. Recently, Assadi and Nazemizadeh [13] studied effect of longitudinal discontinuity of the nanobeam on its size-dependent stability and self-instability with considering the surface elasticity theory. They modeled the nanobeam as a step-wise beam and they derived its governing equation considering compatibility and different boundary conditions.

On the other hand, the nonlocal size-dependent elasticity theory has been presented in the past two decades and has received the attention of many nanotechnology researchers. This theory was first introduced by Eringen [14], and the first application of this theory in modeling nano-scale systems was carried out by Pedison et al. [15]. They modeled a nonlocal nanobeam and indicated that the theory plays an important role in micro/nanotechnology applications. Zhang et al. [16] studied the buckling of a weakened nanobeam subjected to an axial force based on the nonlocal elasticity theory. They considered the effects of weakened joints and size effects on the buckling load of the nanobeam. Nazemizadeh and Bakhtiari-Nejad [17] studied free vibrations of micro/nanobeams including piezoelectric layers. They investigated the size effects on vibrational behavior of nonlocal beams and showed that the nonlocal parameter had a prominent effect on the dynamic behavior of the nanobeam. They also proposed [18] a general formulation for calculating the quality factor of vibrating nanobeams in air environments. Thai et al. [19] presented a formulation for bending and vibration of nanobeams regarding to shear deformation and size effects and considering the nonlocal elasticity theory. They used an analytical method to solve the governing equations. They investigated the size effects on the mechanical behavior of nanobeam. In [20], a perturbation method was employed to solve nonlinear size-dependent vibration of nonlocal two-layered piezo laminated nanobeam. Mawphlang [21] analyzed buckling of non-uniform nanobeams taking into account the nonlocal elastic theory. They derived governing differential equation for nonuniform nanobeam subjected to the axial compressive load and solved the problem numerically by employing the differential transformation method. In [22], nonlocal effects were studied on nonlinear vibration of nanobeams at higher modes of vibration. Recently, Hossein and Lellep [23] investigated natural frequency of stepped nanobeam considering the nonlocal effects and rotary inertia. They used Homotopy perturbation method to solve the governing equations for two steps nanobeam. However, the solution procedure and detail mathematical formulation were ignored.

In this article, the vibration analysis of mass sensor nanobeams is presented with consideration of the longitudinal discontinuity and the nonlocal elasticity theory. The non-uniform and discontinuous model of nanobeams has been inspired by the fact that most micro/nanobeams are designed and fabricated at the narrower end section. Therefore, a discontinuous nanobeam model is considered, which senses the absorbed mass at a desired longitudinal point for mass sensor applications. In order to derive the vibrational equations governing, energy equations of the beam are developed with regard to the discontinuity, and finally, the vibrational equations and boundary conditions of the nonlocal nanobeam are derived according to Hamilton's principle. Then, for the number of longitudinal discontinuities, the same number of responses of mode shapes along the nanobeam is considered by using the analytical solution. Finally, the frequency equation of discontinuous mass sensor nanobeam is obtained as an algebraic relation by applying the compatibility conditions and nonlocal boundary conditions. The natural frequencies in various modes of nanobeam are calculated by solving the frequency response. The effects of different parameters, such as the length of discontinuity, sensed mass, and nonlocal parameters on the frequency behavior of the nanobeam are investigated. Also, the effects of sensed mass and size effects on the shape functions of nanobeam are simulated. These effects are investigated more precisely at higher modes to study the application and efficiency of the mass sensor at higher modes of vibration.

2. Problem Formulation

In this section, firstly, a mass sensor cantilever nanobeam is considered with the ability to sense mass at a desired distance from the clamped end, and then the governing vibrational equation is obtained by using Hamilton's principle. It should be noted that a non-uniform cantilever nanobeam is modeled and stepwise varying properties across the length of the beam is considered in dynamic modeling of the system. This discontinued modeling is originated based on the fact that the mass sensor nanobeams are fabricated wider in the first section, while the end section is designed narrower due to enhance end deflection measurement.

Figure 1 shows a discontinuous cantilever nanobeam.

The characteristics of the nanobeam are as the following: length of the initial section l_1, the distance of the location of discontinuity from the location of sensor mass l_2, the distance of the location of the sensed mass from the free end of the beam l_3, the total length of nanobeam l, width t_i, thickness h_i, and location of the sensed mass l_{Mp}.

Considering the transverse vibrations of the nanobeam along the z-axis, the displacement of any desired point of the nanobeam cross-section in the distance z from the neutral axis is $\vec{r} = [u(x,y,z), v(x,y,z), w(x,y,z)]^{\mathrm{T}}$ and is equal to the following equation:

$$\begin{aligned} u(x,y,z) &= -z\frac{\partial \bar{\bar{w}}}{\partial x} \\ w(x,y,z) &= \bar{w}(x,t) \\ v(x,y,z) &= 0 \end{aligned} \tag{1}$$

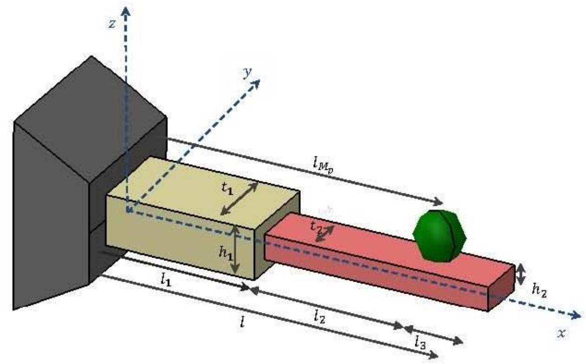

Fig. 1. Nonlocal mass sensor cantilever nanobeam

where $u(x,y,z)$, $v(x,y,z)$, $w(x,y,z)$ and $\overline{w}(x,t)$ are the displacement of the desired point of the nanobeam cross-section in the x-direction, y-direction, z-direction, and the transverse displacement of the neutral axis of nanobeam, respectively.

In order to obtain the governing equations of the system, Hamilton's principle is considered as follows:

$$\int_{t_0}^{t}(\delta T - \delta U + \delta W_{n.c}) = 0 \tag{2}$$

where, T is the kinetic energy, U and $W_{n.c}$ are the potential energy and work of the external force of the system, respectively. The kinetic energy of the system can also be calculated as:

$$T = \frac{1}{2}\iiint_{\bar{V}_b} \bar{\rho}_{b_i}(\frac{\partial \bar{w}}{\partial t})^2 d\bar{V}_{b_i} + \frac{1}{2}\bar{M}_p\left(\frac{\partial \bar{w}(l_{Mp},t)}{\partial t}\right)^2 \tag{3}$$

where, $\bar{\rho}_{b_i}$ and $\bar{V}_{b_i}$ are mass density and the cross-section of nanobeam, respectively, and $\overline{M}_p$ is the absorbed mass on the nanobeam. Then, the kinetic energy can be rewritten by using the Heaviside function:

$$T = \frac{1}{2}\int_0^{\bar{L}}\left\{\begin{aligned}&\bar{\rho}_{b_1}\bar{A}_{b_1}[H(x) - H(x-l_1)]\\ &+\bar{\rho}_{b_2}\bar{A}_{b_2}[H(x-l_1) - H(x-l_2)]\end{aligned}\right\}dx + \frac{1}{2}\bar{M}_p\left(\frac{\partial \bar{w}(l_{Mp},t)}{\partial t}\right)^2 \tag{4}$$

where the Heaviside function $H(x)$ is a non-continuous function whose value is zero for negative input and one for positive input.

The potential energy is also calculated as the following equation:

$$U = \frac{1}{2}\iiint_{V_b} \bar{\sigma}_{xx,b}\varepsilon_{xx}\, d\bar{V}_b \tag{5}$$

where, $\overline{\sigma}_{xx,b}$ is the nonlocal stress along the x-axis. Also, the non-zero term of the nanobeam strain is equal to:

$$\varepsilon_{xx} = -z\frac{\partial^2 \bar{w}(x,t)}{\partial x^2} \tag{6}$$

Moreover, the main point of nonlocal continuum mechanics is that the nonlocal stress tensor at the reference point $\vec{r}$ depends not only on the strain tensor of the same coordinates but also on all points of the body [14]. The basic equation proposed by Eringen in integral form is as the following:

$$\bar{\sigma}_{ij}(\vec{r}) = \int_V \alpha(|\vec{r} - \vec{r}'|)\sigma_{ij}(\vec{r}')d\bar{V}(\vec{r}') \tag{7}$$

where $\overline{\sigma}_{ij}$ is the nonlocal stress tensor, $\alpha(|\vec{r}|)$ indicates to the nonlocal kernel, $\vec{r}$ is the coordinate of the reference point, and $\vec{r}'$ is referred to the coordinate of each point of the body. In addition, σ_{ij} is a local stress tensor that for a homogeneous isotropic object is stated as:

$$\sigma_{ij} = \bar{E}_{ijkl}\varepsilon_{kl} \quad (8)$$

where, $\bar{E}_{ijkl}$ is the elastic stiffness tensor, and ε_{kl} is the strain tensor. Moreover, Eringen showed that a differential form of the nonlocal formulation could be used instead of the integral form (7) as follows [14]:

$$(1-\mu^2\nabla^2)\bar{\sigma}_{ij} = \sigma_{ij} \quad (9)$$

where, ∇^2 is the Laplace operator, and μ is defined as the scaling coefficient, which includes the size-dependent small-scale coefficients. In addition, the nonlocal stress tensor for nanobeam is presented as the following integral equation:

$$\bar{\sigma}_{ij}(\vec{r}) = \int_{\bar{V}} \alpha\left(\left|\vec{r}-\vec{r}'\right|\right)\left(\bar{E}_{ijkl}\varepsilon_{kl}(\vec{r}')\right)d\bar{V} \quad (10)$$

The equation (10) can be converted into the following differential form:

$$(1-\mu^2\nabla^2)\bar{\sigma}_{ij} = \bar{E}_{ijkl}\varepsilon_{kl} \quad (11)$$

And, the one-dimensional form of the differential nonlocal equation can be rewritten as:

$$\left(1-\mu^2\frac{\partial^2}{\partial x^2}\right)\bar{\sigma}_{xx,b} = \bar{E}_b\varepsilon_{xx} \quad (12)$$

where, $\bar{E}_b$ is Young's modulus of the nanobeam.

By placing Eq. 6. in Eq. 5, the following equation is obtained:

$$U = \frac{1}{2}\iiint_{V_b} -z\bar{\sigma}_{xx,b}\frac{\partial^2\bar{w}(x,t)}{\partial x^2}dV_b \quad (13)$$

Also, Eq. 13 can be summarized as follows:

$$U = \frac{1}{2}\int_0^l \left(\bar{M}_{eq}\frac{\partial^2\bar{w}(x,t)}{\partial x^2}\right)dx \quad (14)$$

where, $\bar{M}_{eq}$ is considered as:

$$\bar{M}_{eq} = -[H(x)-H(x-l_1)]\iint_{\bar{A}_{b_1}}\bar{\sigma}_{xx,b}zd\bar{A}_{b_1} - [H(x-l_1)-H(x-l)]\iint_{\bar{A}_{b_2}}\bar{\sigma}_{xx,b}zd\bar{A}_{b_2} \quad (15)$$

Moreover, the work of the external force is also calculated as follows:

$$W_{n.c} = \frac{1}{2}\int_0^l \bar{f}\bar{w}(x,t)dx \quad (16)$$

where, $\bar{f}$ is the external force applied to the nanobeam.

Now by submitting Eqs. (3), (12), and (14) in the Hamilton principle (2), the equations of motion and boundary conditions can be obtained as the following relations:

$$\bar{\rho}_{eq}\bar{A}_{eq}\frac{\partial^2\bar{w}(x,t)}{\partial t^2} + \bar{f} = \frac{\partial^2\bar{M}_{eq}}{\partial x^2} \quad (17)$$

$$\begin{aligned} &x=0: \\ &\bar{w}(0,t)=0 \ \ and \ \ \frac{\partial\bar{w}(0,t)}{\partial x}=0 \\ &x=l: \\ &M_{eq}=0 \ \ and \ \ \frac{\partial M_{eq}}{\partial x}=0 \end{aligned} \quad (18)$$

where the equivalent mass of the system is expressed as follows:

$$\bar{\rho}_{eq}\bar{A}_{eq} = \bar{\rho}_{b_1}\bar{A}_{b_1}[H(x)-H(x-l_1)] + \rho_{b_2}\bar{A}_{b_2}[H(x-l_1)-H(x-l)] + \bar{M}_p(x-l_{Mp}) \quad (19)$$

Besides, the following equation will be obtained by integrating the Eqs. (12) over the cross-section of the nanobeam:

$$M_{eq} - \mu^2\frac{\partial^2 M_{eq}}{\partial x^2} = -\bar{E}_{eq}\bar{I}_{eq}\frac{\partial^2\bar{w}}{\partial x^2} \quad (20)$$

where the following relations are considered:

$$\bar{E}_{eq}\bar{I}_{eq} = \bar{E}_{b_1}I_{b_1}[H(x)-H(x-l_1)] + E_{b_2}\bar{I}_{b_2}[H(x-l_1)-H(x-\bar{L})] \quad (21)$$

$$\{\bar{I}_{b1},\bar{I}_{b2}\} = \iint_{\{\bar{A}_{b1},\bar{A}_{b2}\}} z^2\{d\bar{A}_{b1},d\bar{A}_{b2}\} \quad (22)$$

By submitting Eq. 16. in Eq. 19. the following equation will be obtained:

$$M_{eq} = -\bar{E}_{eq}\bar{I}_{eq}\frac{\partial^2 w(x,t)}{\partial x^2} + \mu^2\left[\bar{\rho}_{eq}\bar{A}_{eq}\frac{\partial^2\bar{w}(x,t)}{\partial t^2} + \bar{f}\right] \quad (23)$$

Furthermore, the governing equation and boundary conditions of the nanobeam can be presented as follows by using Eqs. 18, 19, and 23

$$\begin{aligned} \left(1-\mu^2\frac{\partial^2}{\partial x^2}\right)&\left(\bar{\rho}_{eq}\bar{A}_{eq}\frac{\partial^2\bar{w}(x,t)}{\partial t^2}\right) \\ &+\frac{\partial^2}{\partial x^2}\left(\bar{E}_{eq}\bar{I}_{eq}\frac{\partial^2\bar{w}(x,t)}{\partial x^2}\right) \\ &+\bar{f}\left(1-\mu^2\frac{\partial^3\bar{w}(x,t)}{\partial x^2\partial t}\right) \\ &=0 \end{aligned} \quad (24)$$

$$\begin{aligned} &x=0: \\ &\bar{w}(0,t)=0 \ \ and \ \ \frac{\partial\bar{w}(0,t)}{\partial x}=0 \\ &x=l: \\ &\bar{E}_{eq}\bar{I}_{eq}\frac{\partial^2\bar{w}}{\partial x^2} - \mu^2\bar{\rho}_{eq}\bar{A}_{eq}\frac{\partial^2\bar{w}}{\partial t^2}=0 \\ &\frac{\partial}{\partial x}\left[\bar{E}_{eq}\bar{I}_{eq}\frac{\partial^2\bar{w}}{\partial x^2} - \mu^2\bar{\rho}_{eq}\bar{A}_{eq}\frac{\partial^2\bar{w}}{\partial t^2}\right]=0 \end{aligned} \quad (25)$$

The boundary conditions presented in Eq. 25. are related to zero displacement and zero slope at $x = 0$, as well as to zero nonlocal torque and zero transverse shear force of at x = *l*.

3. Analytical Solution

In the previous section, the governing equations and boundary conditions of the nanobeam were obtained. In order to analytically solve the vibration equation of the nanobeam with the sensed mass at the desired distance, the beam is divided into three sections: 1) from the fixed end to the location of cross-section discontinuity, 2) from the location of cross-section discontinuity to the sensed mass, 3) from the absorbed mass to the free end of the beam. Therefore, Eq. 24 is rewritten as the following:

$$\begin{aligned}
&0 < x < l_1: \\
&\bar{\rho}_{eq,1}\bar{E}_{eq,1}\left(1-\mu^2\frac{\partial^2}{\partial x^2}\right)\left(\frac{\partial^2\bar{w}_1(x,t)}{\partial t^2}\right) \\
&\qquad +\bar{E}_{eq,1}\bar{I}_{eq,1}\frac{\partial^4\bar{w}_1(x,t)}{\partial t^4}=0 \\
&l_1 < x < l_{Mp}: \\
&\bar{\rho}_{eq,2}\bar{E}_{eq,2}\left(1-\mu^2\frac{\partial^2}{\partial x^2}\right)\left(\frac{\partial^2\bar{w}_2(x,t)}{\partial t^2}\right) \\
&\qquad +\bar{E}_{eq,2}\bar{I}_{eq,2}\frac{\partial^4\bar{w}_2(x,t)}{\partial t^4}=0 \\
&l_{M_p} < x < l: \\
&\bar{\rho}_{eq,3}\bar{E}_{eq,3}\left(1-\mu^2\frac{\partial^2}{\partial x^2}\right)\left(\frac{\partial^2\bar{w}_3(x,t)}{\partial t^2}\right) \\
&\qquad +\bar{E}_{eq,3}\bar{I}_{eq,3}\frac{\partial^4\bar{w}_3(x,t)}{\partial t^4}=0
\end{aligned} \tag{26}$$

Furthermore, the boundary conditions at both ends of the nanobeam and the compatibility conditions at the location of the cross-section discontinuity and absorbed mass are expressed as:

$$\begin{aligned}
&\bar{x}=0: \\
&\bar{w}_1(0,t)=0 \ and \ \frac{\partial\bar{w}_1(0,t)}{\partial\bar{x}}=0 \\
&x=l: \\
&\bar{E}_{eq,3}\bar{I}_{eq,3}\frac{\partial^2\bar{w}_3(l,t)}{\partial x^2}-\mu^2\bar{\rho}_{eq,3}\bar{A}_{eq,3}\frac{\partial^2\bar{w}_3(l,t)}{\partial t^2}=0 \\
&\bar{E}_{eq,3}\bar{I}_{eq,3}\frac{\partial^3\bar{w}_3(l,t)}{\partial x^3}-\mu^2\bar{\rho}_{eq,3}\bar{A}_{eq,3}\frac{\partial^3\bar{w}_3(l,t)}{\partial x\partial t^2}=0 \\
&x=l_1: \\
&\bar{w}_1(l_1,t)=\bar{w}_2(l_1,t) \\
&\frac{\partial\bar{w}_1(l_1,t)}{\partial x}=\frac{\partial\bar{w}_2(l_1,t)}{\partial x} \\
&\bar{E}_{eq,1}\bar{I}_{eq,1}\frac{\partial^2\bar{w}_1(l_1,t)}{\partial x^2}-\bar{E}_{eq,2}\bar{I}_{eq,2}\frac{\partial^2\bar{w}_2(l_2,t)}{\partial x^2} \\
&-\mu^2\bar{\rho}_{eq,1}\bar{A}_{eq,1}\frac{\partial^2\bar{w}_1(l_1,t)}{\partial t^2} \\
&\qquad +\mu^2\bar{\rho}_{eq,2}A_{eq,2}\frac{\partial^2\bar{w}_2(l_2,t)}{\partial t^2}=0 \\
&\bar{E}_{eq,1}\bar{I}_{eq,1}\frac{\partial^3\bar{w}_1(l_1,t)}{\partial x^3}-\bar{E}_{eq,2}\bar{I}_{eq,2}\frac{\partial^3\bar{w}_2(l_2,t)}{\partial x^3} \\
&-\mu^2\bar{\rho}_{eq,1}\bar{A}_{eq,1}\frac{\partial^3\bar{w}_1(l_1,t)}{\partial x\partial t^2}+\mu^2\bar{\rho}_{eq,2}A_{eq,2}\frac{\partial^3\bar{w}_2(l_2,t)}{\partial x\partial t^2}=0 \\
&x=l_{Mp}: \\
&\bar{w}_2(l_{Mp},t)=\bar{w}_3(l_{Mp},t) \\
&\frac{\partial\bar{w}_2(l_{Mp},t)}{\partial x}=\frac{\partial\bar{w}_3(l_{Mp},t)}{\partial x} \\
&\bar{E}_{eq,2}\bar{I}_{eq,2}\frac{\partial^2\bar{w}_2(l_{Mp},t)}{\partial x^2}-\mu^2\bar{\rho}_{eq,2}\bar{A}_{eq,2}\frac{\partial^2\bar{w}_2(l_{Mp},t)}{\partial t^2} \\
&-\bar{E}_{eq,3}\bar{I}_{eq,3}\frac{\partial^2\bar{w}_3(l_{Mp},t)}{\partial x^2}+\mu^2\bar{\rho}_{eq,3}\bar{A}_{eq,3}\frac{\partial^2\bar{w}_3(l_{Mp},t)}{\partial t^2} \\
&\qquad =0 \\
&\bar{E}_{eq,2}\bar{I}_{eq,2}\frac{\partial^3\bar{w}_2(l_{Mp},t)}{\partial x^3}-\mu^2\bar{\rho}_{eq,2}\bar{A}_{eq,2}\frac{\partial^3\bar{w}_2(l_{Mp},t)}{\partial x\partial t^2} \\
&-M_p\frac{\partial^2\bar{w}_2(l_{Mp},t)}{\partial t^2}-\bar{E}_{eq,3}\bar{I}_{eq,3}\frac{\partial^3\bar{w}_3(l_{Mp},t)}{\partial x^3} \\
&+\mu^2\bar{\rho}_{eq,3}\bar{A}_{eq,3}\frac{\partial^3\bar{w}_3(l_{Mp},t)}{\partial x\partial t^2}=0
\end{aligned} \tag{27}$$

In general, the vibrational response of the system is considered to equal $\overline{w}(x,t)=\overline{w}(x)e^{i\omega t}$, and in order to solve the vibrational equations, the shape function response of each section is equal to [17]:

$$\bar{W}_i(x)=\chi_{1,i}\cos(\eta_i x)+\chi_{2,i}\sin(\eta_i x)+\chi_{3,i}\cos(\lambda_i x)+\chi_{4,i}\sin(\lambda_i x) \tag{28}$$

where, $\chi_{1,i}$ is the unknown coefficient. Also, η_i and γ_i are respectively the function of natural frequency and geometrical characteristic of the system and are stated as:

$$\begin{aligned}
\eta_i &= \sqrt{a_i\omega^2+\sqrt{(a_i\omega^2)^2+b_i\omega^2}} \\
\lambda_i &= \sqrt{-a_i\omega^2+\sqrt{(a_i\omega^2)^2+b_i\omega^2}}
\end{aligned} \tag{29}$$

where, a_i and b_i can be calculated from the following equations [17]:

$$\begin{aligned}
a_i &= \frac{\left(\mu^2\bar{\rho}_{eq,i}\bar{A}_{eq,i}\right)}{\left(2\bar{E}_{eq,i}\bar{I}_{eq,i}\right)} \\
b_i &= \frac{\left(\bar{\rho}_{eq,i}\bar{A}_{eq,i}\right)}{\left(\bar{E}_{eq,i}\bar{I}_{eq,i}\right)}
\end{aligned} \tag{30}$$

Now, if the boundary conditions and compatibility conditions are submitted in the Eq. 28 the frequency matrix is obtained. The natural frequencies and mode shapes of the system can also be obtained by solving the frequency equation.

4. Simulations and Results

In this section, the frequency analysis of the mass sensor nanobeam at higher modes is simulated. The physical and geometrical characteristics of the nanobeam are listed in Table 1.

Table 1. mass sensor nanobeam Characteristics

Physical characteristics			Geometric Specification (nm)				
	$\rho\left({}^{kg}/_{m^3}\right)$	E(Gpa)	l_1	l_2	t_1	h_1	h_2
sio_2	2330	107	60	30	20	10	5

Table 2. comparison of the first dimensionless natural frequency ϖ

R	μ	Current research	Reference [15]
0	0	1.8751	1.8751
	0.1	1.8792	1.8791
	0.2	18919	1.8917

Firstly, to verify the presented solution, the first dimensionless natural frequency of a cantilever nanobeam is compared with the values presented in [15]. The case study is a uniform nanobeam without any sensed mass. It should be noted the dimensionless natural frequency of the uniform nanobeam is defined as

$$\varpi = \omega l^2 \sqrt{\frac{\bar{\rho}_{eq}\bar{A}_{eq}}{\bar{E}_{eq}\bar{I}_{eq}}}.$$

Also, in table 3, the natural frequency of a classical beam for different attached mass is compared with the frequencies presented in [24] where $R = \frac{M_p}{\bar{\rho}_{eq}\bar{A}_{eq}}$ is defined. As it can be seen, the results of the present study are in good agreement with the results presented in [15] and [24], and hence the proposed analytical solution for vibration analysis of the nanobeam can be confidently implemented. However, a bit differences in results can be related to numerical solution and rounding.

Furthermore, in the first simulation, the effect of the exact modeling of the nanobeam on its frequency behavior is investigated. For this purpose, the nonlocal discontinuous nanobeam as a precise model is compared with the inaccurate models: the local discontinuous beam, nonlocal uniform beam, and local uniform beam. It is considered that the sensed mass is located at the free end of the nanobeam, and the natural frequency of the beam is calculated.

In Table (4), the first natural frequency and its relative error for different models compared to the exact model (non-local discontinuous beam) has been calculated in MHz taking into account the nonlocal parameter to be $\mu = 0.1$.

Table 3. comparison of the first dimensionless natural frequency

R	Frequency	Current research	Reference [24]
0.01	First	1.8568	1.852
	Second	4.6498	4.650
0.1	First	1.7228	1.723
	Second	4.3996	4.399
1	First	1.2480	1.248
	Second	4.0312	4.041

Table 4. First natural frequency (MHz) of the nanobeam considering different models

	First Frequency			
	R = 0		R = 0.5	
	Value	Error (%)	Value	Error (%)
Nonlocal stepped beam	1.261	-	0.654	-
Classic stepped beam	1.249	0.95	0.651	0.458
Nonlocal uniform beam	1.357	7.6	0.776	18.65
Classic uniform beam	1.352	7.21	0.775	18.50

It can be seen in Table (4) that the effect of discontinuity is essential in the exact modeling of the nanobeam. Therefore, the relative error caused by applying the continuous model is not negligible, compared to the discontinuous model, which shows the importance of the present work for the exact modeling of the beam.

In another simulation, the natural frequency of the system caused by changing the location of the sensed mass is investigated. Besides, in Table 5, the first and second natural frequencies of the nanobeam are calculated in MHz and presented for different locations of the sensed mass. It should be noted that $\bar{L}_M = (l_1 + \Delta l_2))/l$.

Table 5. Effect of the sensed mass position on the first and second natural frequencies (MHz) of the mass sensor nanobeam

μ	Δ	R	ω_1	ω_2
0	0.25	0.25	1.221	4.936
		0.5	1.193	4.302
	0.5	0.25	0.976	6.066
		0.5	0.828	6.063
0.1	0.25	0.25	1.232	4.732
		0.5	1.203	4.178
	0.5	0.25	0.981	5.661
		0.5	0.831	5.658

According to Table 5, in the first vibration mode, the natural frequency is reduced by changing the position of the sensed mass toward the free end of the nanobeam and increasing the attached mass. The reason is that in the first vibrational mode, with increasing the mass and its movement toward the free end, the inertia increases at the end of the beam and causes the reduction of the natural frequency. Besides, the effect of increasing the nonlocal term and size effects on the shift of the first natural frequency of the nanobeam is negligible, and these effects decrease with increasing the ratio of absorbed mass. However, in the second vibrational mode, since the node of the second shape function is adjacent to $\Delta = 0.75$, increasing the absorbed mass in this position causes a smaller decrease in the natural frequency compared to other positions of the mass. Also, by increasing the vibrational modes, the effect of the nonlocal term and size effects on the frequency becomes more important and decreases the natural frequency of the beam. The reason is that in the classical elasticity theory, it is assumed that the atoms of bodies are rigidly bonded together; however, in the nonlocal elasticity theory, the atoms of bodies are linked together in an elastic environment matrix with an assumption of spring contact. Therefore, in the nonlocal elasticity theory, the stiffness of nanostructure is lower, and the natural frequency is reduced. Furthermore, the effect of nonlocal terms at the higher natural frequencies is more prominent. It may be explained by the reality that wavelengths are decreased for higher modes and the stronger interactions between atoms lead to increasing of the nonlocal effect.

In another study, the effect of nonlocal parameters on the mode shapes of the mass sensor nanobeam is shown for different absorbed masses at its end. Fig. 2 shows the shape function of the first mode of the beam:

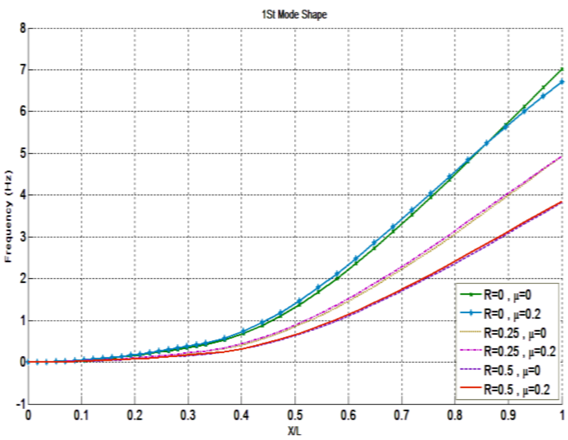

Fig. 2. The first mode shape of the nanobeam for different sensed mass

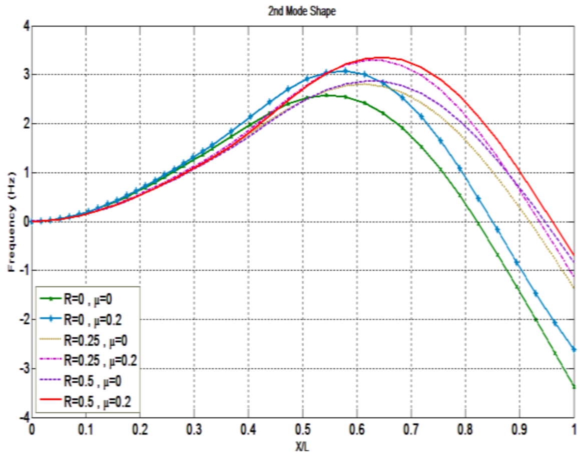

Fig. 3. The second mode shape of the nanobeam for different sensed mass

As seen in Fig. 2, increasing the nonlocal term and size effects slightly increases the amplitude of the first mode of the nanobeam. However, size effects decrease with increasing the sensed mass. In fact, the nonlocal effects are not dominant at the first mode of vibration. On the contrary, the amplitude of the mode shape decreases with increasing the absorbed mass. The reason is that as the sensed mass increases, the total inertia of the mass sensor nanobeam increases and leads to a reduction of the amplitude of the end of the nanobeam.

Furthermore, the shape function of the second mode of the sensor nanobeam for different absorbed mass at the end of the beam is depicted in Fig. 3.

As can be observed in Fig. 3, increasing the nonlocal term in the second vibrational mode increases the amplitude of the mode shape. The reason for the increase in the amplitude of mode shape is that the nonlocal term reduces the stiffness of the nanobeam and thus increases the vibrational amplitude. Also, the amplitude of the mode shape decreases with increasing the absorbed mass. It is also observed that by increasing the sensed mass, the effect of the nonlocal term on the mode shape of the nanobeam decreases.

In another simulation, according to Table 6, the frequency behavior of the classical and nonlocal nanobeam is investigated for different thickness ratios $\bar{h} = \frac{h_2}{h_1}$.

As is evident in Table 6, increasing the thickness of the nanobeam increases the natural frequency because increasing the thickness increases the mass and stiffness of the nanobeam simultaneously, but its effect on the stiffness is higher than on the structural mass. On the other hand, as this term increases, the ratio of the frequency reduction is decreased for the sensed mass nanobeam.

Table 6. First natural frequency (MHz) of the nanobeam considering different models

μ	R	h̄	ω_1	ω_2
0	0	0.3	0.869	4.924
		0.6	1.343	6.485
	0.25	0.3	0.553	3.977
		0.6	0.896	5.387
0.1	0	0.3	0.878	4.458
		0.6	1.354	6.072
	0.25	0.3	0.556	3.621
		0.6	0.900	5.072

In another study, the effect of the sensed mass and nonlocal term on the natural frequency shift of the nanobeam is investigated at the first and second vibrational modes. Fig. 4 indicates the frequency shift $\Delta f = f_1 - f_0$, where f_1 is the frequency of beam without absorbing the sensed mass, and f_0 is the beam frequency with mass absorption.

As can be seen in Fig. 4 the frequency shift of the nanobeam sensor increases with the increase of the absorbed mass. Furthermore, in the first mode of vibration, the effect of nonlocal term and size effects on frequency shifts are negligible.

Also, the shift of the second mode of the frequency of the nanobeam relative to sensed mass is indicated in Fig. 5.

As shown in Fig. 5, the frequency shift increases with the increase of the sensed mass at the second vibrational mode, but the slope of this increment is decreasing relative to the absorbed mass. In the second vibrational mode, the nonlocal term and size effects reduce the mass sensing of the nanobeam. On the other hand, the sensitivity and frequency change of nanobeam in the second vibrational mode was greater than that of the first vibrational mode; hence, it is recommended to use the mass sensor nanobeam at higher modes.

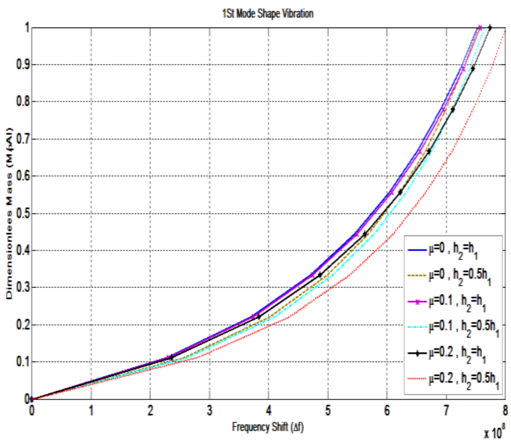

Fig. 4. shift of the first natural frequency of the mass sensor nanobeam

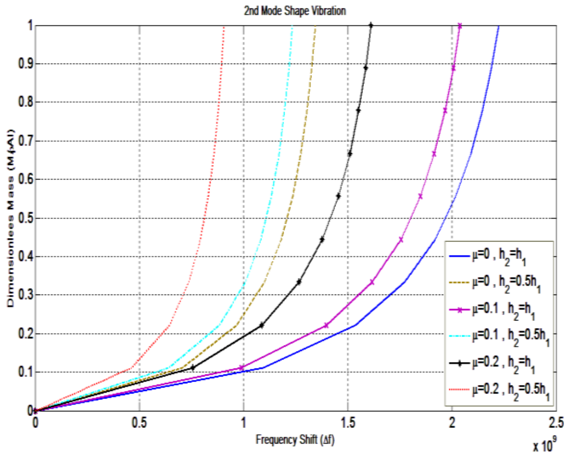

Fig. 5. The shift of the second natural frequency of the mass sensor nanobeam

5. Conclusions

In this paper, the precise modeling of the nanobeam has been carried out considering discontinuity based on the size-dependent nonlocal elasticity theory. The vibrational equations and boundary conditions of the mass sensor nanobeam have been derived by using Hamilton's principle. Then, the frequency equation of the discontinuous nanobeam has been obtained as an algebraic relation by using an analytical solution and considering the sensed mass. The effect of various parameters such as length of discontinuity, sensed mass, and nonlocal parameters on the frequency behavior of the nanobeam have been investigated. The results showed that the effect of discontinuity on the precise modeling of the nanobeam is of great importance and should be taken into account; however, increasing the sensed mass has reduced the relative error of the modeling. The effect of the nonlocal term and size effects are important at higher vibrational modes and should be considered in the nanobeam modeling. Besides, by changing the position of the sensed mass toward the free end of the nanobeam, the natural frequency is reduced, but its sensing sensitivity increases. Increasing the thickness of the nanobeam increases the stiffness of the structure and its natural frequency but decreases the sensitivity of the mass sensor nanobeam.

References

[1] Sadeghzadeh, S., 2018. Geometric Effects on Nanopore Creation in Graphene and on the Impact-withstanding Efficiency of Graphene Nanosheets. *Mechanics of Advanced Composite Structures*, *5*(1), pp.91-102.

[2] Bakhtiari-Nejad, F. and Nazemizadeh, M., 2016. Size-dependent dynamic modeling and vibration analysis of MEMS/NEMS-

based nanomechanical beam based on the nonlocal elasticity theory. *Acta Mechanica*, *227*(5), pp.1363-1379.

[3] Rostamiyan, Y., 2017. Improving Mechanical Properties of Nanocomposite-based Epoxy by High-impact Polystyrene and Multiwalled Carbon Nanotubes: Optimizing by a Mixture Design Approach. *Mechanics of Advanced Composite Structures*, *4*(1), pp.33-45.

[4] Taheri M., 2019. Investigation and Sensitivity Analysis of Dimensional Parameters and Velocity in the 3D Nanomanipulation Dynamics of Carbon Nanotubes Using Statistical Sobol Method. *Modares Mechanical Engineering*, 19(1), pp. 125-135.

[5] Korayem, M.H., Hezaveh, H.B. and Taheri, M., 2014. Dynamic modeling and simulation of rough cylindrical micro/nanoparticle manipulation with atomic force microscopy. *Microscopy and Microanalysis*, *20*(6), pp.1692-1707.

[6] Rostamiyan, Y., 2017. Improving Mechanical Properties of Nanocomposite-based Epoxy by High-impact Polystyrene and Multiwalled Carbon Nanotubes: Optimizing by a Mixture Design Approach. *Mechanics of Advanced Composite Structures*, *4*(1), pp.33-45.

[7] Kabiri, A. and Sadeghzadeh, S., 2018. Sensitivity Analysis of Fiber-Reinforced Lamina Micro-Electro-Mechanical Switches with Nonlinear Vibration Using a Higher Order Hamiltonian Approach. *Mechanics of Advanced Composite Structures*, *5*(1), pp.25-39.

[8] Jiang, L.Y. and Yan, Z., 2010. Timoshenko beam model for static bending of nanowires with surface effects. *Physica E: Low-dimensional systems and Nanostructures*, 42(9), pp.2274-2279.

[9] Elishakoff, I., Challamel, N., Soret, C., Bekel, Y. and Gomez, T., 2013. Virus sensor based on single-walled carbon nanotube: improved theory incorporating surface effects. *Philosophical Transactions of the Royal Society A: Mathematical, Physical and Engineering Sciences*, *371*(1993), p.20120424.

[10] Jalali, M.H., Zargar, O. and Baghani, M., 2019. Size-dependent vibration analysis of FG microbeams in thermal environment based on modified couple stress theory. *Iranian Journal of Science and Technology, Transactions of Mechanical Engineering*, *43*(1), pp.761-771.

[11] Khorshidi K. and Fallah A. 2017. Free vibration analysis of size-dependent, functionally graded, rectangular nano/micro-plates based on modified nonlinear couple stress shear deformation plate theories. *Mechanics of Advanced Composite Structures*, *4*(2), pp. 127-137.

[12] Fallah A. and Khorshidi K. 2019. The effect of nonlinear temperature distribution on the vibrational behavior of a size-dependent FG laminated rectangular plates undergoing prescribed overall motion. *Polymer Composites*, *40*(2), pp. 766-778.

[13] Assadi A., Nazemizadeh M. 2020. Size effects on stability and self-instability of non-uniform nanobeams with consideration of surface effects. *Micro & Nano Letters*. Doi: 10.1049/mnl.2020.0262.

[14] Eringen, A.C., 1977. Screw dislocation in non-local elasticity. *Journal of Physics D: Applied Physics*, *10*(5), p.671

[15] Peddieson, J., Buchanan, G.R. and McNitt, R.P., 2003. Application of nonlocal continuum models to nanotechnology. *International Journal of Engineering Science*, 41(3-5), pp.305-312.

[16] Zhang, Y., Pang, M. and Chen, W., 2013. Non-local modelling on the buckling of a weakened nanobeam. *Micro & Nano Letters*, *8*(2), pp.102-106.

[17] Nazemizadeh, M. and Bakhtiari-Nejad, F., 2015. Size-dependent free vibration of nano/microbeams with piezo-layered actuators. *Micro & Nano Letters*, *10*(2), pp.93-98.

[18] Nazemizadeh, M. and Bakhtiari-Nejad, F., 2015. A general formulation of quality factor for composite micro/nano beams in the air environment based on the nonlocal elasticity theory. *Composite Structures*, *132*, pp.772-783.

[19] Thai, S., Thai, H.T., Vo, T.P. and Patel, V.I., 2018. A simple shear deformation theory for nonlocal beams. *Composite Structures*, *183*, pp.262-270.

[20] Nazemizadeh M., Bakhtiari-Nejad F., Assadi A. and Shahriari B. 2020. Size-dependent nonlinear dynamic modeling and vibration analysis of piezo-laminated nanomechanical resonators using perturbation method. *Archive of Applied Mechanics*, pp. 1-14.

[21] Mawphlang B.L., 2020. Buckling analysis of nonuniform nanobeams using nonlocal elastic theory and differential transformation method. *Condensed Matter Physics Research Center, 11*, p. 14.

[22] Nazemizadeh M., Bakhtiari-Nejad F. and Assadi A. 2020. Nonlinear vibration of piezoelectric laminated nanobeams at higher modes based on nonlocal piezoelectric theory. *Acta Mechanica*, *231*(10), pp. 4259-4274.

[23] Hossain M. and Lellep J. 2020. The effect of rotatory inertia on natural frequency of cracked and stepped nanobeam. *Engineering Research Express*, *2*(3), p. 035009.

[24] Rao, S.S., 2007. *Vibration of continuous systems* (Vol. 464). New York: Wiley.